Alternative splicing variant of *RHBDD2* is associated with cell stress response and breast cancer progression

ROMINA CANZONERI, MARTÍN ENRIQUE RABASSA, AGUSTINA GURRUCHAGA, VALERIA FERRETTI, SABINA PALMA, MARINA ISLA-LARRAIN, MARÍA VIRGINIA CROCE, EZEQUIEL LACUNZA and MARTÍN CARLOS ABBA

Basic and Applied Immunological Research Center (CINIBA), School of Medical Sciences, National University of La Plata (UNLP), La Plata, Buenos Aires 1900, Argentina

DOI: 10.3892/or_xxxxxxxx

Abstract. RHBDD2 is an intramembrane pseudoprotease member of the Rhomboid superfamily. Our previous studies in breast and colorectal cancer indicate an association between *RHBDD2* overexpression and advanced tumor stages. Two alternative transcriptional variants have been described for *RHBDD2*, which would be encoding for different RHBDD2 protein isoforms. The expression of these *RHBDD2* variants/isoforms and its association with breast cancer was the focus of this study. First, expression of *RHBDD2* splicing variants was evaluated in normal and breast tumor samples. *RHBDD2* variant 2 overexpression was detected in tumors in respect to normal breast tissues at the mRNA and protein levels (P<0.05). Moreover, *RHBDD2* variant 2 expression was associated with poor prognostic factors such as basal-like intrinsic subtype (P<0.05), high proliferation (P<0.01) and long-term risk-of-recurrence (P<0.01) scores. Second, the expression of both variants was evaluated under nutritional-deprived conditions in breast cancer cell lines. Results demonstrated that *RHBDD2* splicing was switched from mRNA variant 1 to variant 2 in association with a significant increment of protein isoform B in response to glucose starvation treatment. Therefore, we propose that the switch from the *RHBDD2* variant 1, expressed in normal epithelial cells, to variant 2 occurs as an adaptive phenotype to bypass the stressful tumor microenvironment and promote tumor progression. Finally, the RHBDD2 subcellular localization was corroborated at the Golgi apparatus and their associated v-SNARE transport vesicles, suggesting a putative new role for RHBDD2 in the protein trafficking of human breast cancer cells.

Correspondence to: Dr Martín Carlos Abba, Basic and Applied Immunological Research Center (CINIBA), School of Medical Sciences, National University of La Plata (UNLP), 60 and 120 Street, La Plata, Buenos Aires 1900, Argentina
E-mail: mcabba@gmail.com

Key words: RHBDD2, breast cancer, protein isoform, subcellular localization

Introduction

Rhomboid genes encode the most distributed and evolutionarily conserved polytopic intramembrane proteins (1). This superfamily comprises active intramembrane serine proteases that can activate or transactivate the epidermal growth factor receptor (EGFR) signaling pathway and a group of non-catalytic members with diverse cellular functions (1). The human genome contains 14 rhomboid genes that can be grouped into five rhomboid proteases (*RHBDL1/2/3/4* and *PARL*) and nine pseudoproteases (*iRhom1/2*, *Derlin1/2/3*, *RHBDD2/3*, *UBAC2* and *TMEM115*) (2). Previous studies have demonstrated that rhomboid proteases and pseudoproteases are involved in several cellular processes such as cell proliferation, apoptosis, endoplasmic reticulum (ER) stress and EGFR activation. Rhomboids have also been associated with human diseases, such as neurodegenerative conditions, as well as cancer (2).

RHBDD2 pseudoprotease has been found overexpressed in advanced-stage breast and colorectal cancers (3-6). Although the particular *RHBDD2* function has not yet been assessed, its expression has been associated with breast cancer cell migration, proliferation, and cellular response to ER stress (7). A previous study has suggested the existence of two human *RHBDD2* transcriptional variants which are differentiated by the alternative splicing of exon II in the mature mRNA (4). The *RHBDD2* mRNA variant 1 (*RHBDD2-1)* encodes a protein known as isoform A, while *RHBDD2* variant 2 (*RHBDD2-2*) encodes a shorter protein called isoform B (4).

It is known that a subtle balance between splicing variants is crucial to cellular homeostasis, while the unbalanced expression of splicing variants contributes to cancer development (8). The expression pattern of specific variants of numerous genes (eg. *BRCA1/2* genes) is altered during oncogenesis giving the cell an adaptive phenotype to the changing tumor environment (9,10). The switch between isoforms is regulated by different genetics and environmental factors finally determining the tumor phenotype (11,12).

In the present study, we analyzed the expression of the *RHBDD2* splicing variants in neoplastic and normal breast samples, as well as in breast cancer cell lines under nutritional stress conditions. In addition, we determined the RHBDD2 protein subcellular localization in breast cancer cells.

Materials and methods

Breast tissue samples. Breast tissue specimens were obtained from different hospitals and medical centres associated with the School of Medical Sciences of the National University of La Plata. Twenty-three breast primary tumor samples (all invasive ductal carcinomas), as well as 12 normal mammary gland samples obtained from aesthetic mammoplasties were studied. All samples were obtained from female patients ranging from 28 to 89 years old, during the period from February 2011 to October 2015.

Breast cancer cell line culture and glucose starvation (GS) assay. The human MCF7, T47D and MDA-MB-231 breast cancer cell lines were purchased from the ATCC® Bioresource Center (Manassas, VA, USA). Cells were cultured in Dulbecco's modified Eagle's medium (DMEM) (D7777; Sigma-Aldrich; Merck KGaA, Darmstadt, Germany) with 10% fetal bovine serum (FBS; Natocor, Villa Carlos Paz, Argentina), 100 U/ml penicillin and 100 μg/ml streptomycin (P0781; Sigma-Aldrich; Merck KGaA) at 37˚C in humidified atmosphere with 5% CO_2. MCF7 and T47D cell lines were also cultured under glucose starvation (GS) conditions. Briefly, cells were cultured on a 6-well plate to 70% confluence in complete DMEM (D7777) with glucose as described above. Then, the medium was replaced by incomplete DMEM medium (D5030; Sigma-Aldrich; Merck KGaA) without glucose and FBS, supplemented with 100 U/ml penicillin and 100 μg/ml streptomycin. Cells were maintained under GS condition for 3, 6, 9 and 12 h. Control cells were cultured in complete DMEM. At each time point, the cells were harvested and total protein and RNA were isolated.

Protein and total RNA were isolated using TRI Reagent™ solution (Thermo Fisher Scientific, Inc., Waltham, MA, USA) according to the manufacturer's protocol. The SuperScript™ Reverse Transcriptase kit (Thermo Fisher Scientific, Inc.) was used for cDNA synthesis according to the manufacturer's protocol.

Gene expression analysis. Total *RHBDD2* and *RHBDD2-2* (splicing variant 2) expression levels were analyzed by RT-qPCR using the StepOne™ Real-Time PCR System and associated Software v2.3 (Thermo Fisher Scientific, Inc.). In addition, genes involved in cell stress response were evaluated: *DDIT3* mRNA expression was measured as reference for cell GS response (13), while *HSPA5* and *CALR* were evaluated for ER cell stress (14,15). Gene expression levels were calculated by the $2^{-\Delta Cq}$ method (16), using as reference *rRNA18S*. The SYBR™ Select Master Mix (Thermo Fisher Scientific, Inc.) was used for RT-qPCR reaction solution, according to manufacturer's protocol. The following primers were used: *total RHBDD2* (Fw: 5'-ggtgtttggcatggttgtg-3', Rv: 5'-cgatggaatagcagtaggtga-3'); *RHBDD2-2* (Fw: 5'-attacagcagaggagactgg-3', Rv: 5'-gatgtaggttaccagcctgt-3'); *DDIT3* (Fw: 5'-agccaaaatcagagctggaa-3' and Rv: 5'-tggatcagtctggaaaagca-3); *HSPA5* (Fw: 5'-cacagtggtgcctaccaaga-3' and Rv: 5'-tgtcttttgtcaggggtc ttt-3'); *CALR* (Fw: 5'-acaaccccgagtattctccc-3' and Rv: 5'-tgt caaagatggtgccagac-3') and *rRNA18S* (Fw: 5'-gtaacccgttgaa ccccatt-3', Rv: 5'-ccatccaatcggtagtagcg-3'). RT-PCR thermal profile was as follows: 5 min at 95˚C, 40 cycles of 40 sec at 95˚C-30 sec at 55˚C (for all primer pairs)-30 sec at 72˚C, and a final cycle at 95˚C for 1 min-55˚C for 30 sec and 96˚C for 30 sec was added.

RHBDD2 isoform analysis in breast cancer cell lines and tissue samples. The *RHBDD2* splicing variants and protein isoform expression were evaluated in breast cancer cell lines and breast normal and tumor samples selected for showing *RHBDD2* mRNA expression. Total *RHBDD2* and *RHBDD2-2* mRNA expression were analyzed by RT-qPCR, using the primers mentioned above. We also evaluated by direct sequencing the *RHBDD2* splicing variant RT-PCR products obtained with the primer pair: Fw: 5'-tgaagtccgaggccctt-3' (complementary to exon I) and Rv: 5'-caaagcgccagatgatgata-3' (complementary to exon III).

The RHBDD2 protein isoforms were detected by SDS-PAGE followed by Western-blot analysis. Total protein was isolated from human cell lines and breast samples with TRI Reagent™ Solution (Thermo Fisher Scientific, Inc.) according to the manufacturer's protocol. The primary antibody: rabbit anti-RHBDD2 (1:1,000; cat. no. TA306891; Origene, Rockville, MD, USA) was incubated overnight at 4˚C. The antibody target sequence is located at the C-terminal domain of both RHBDD2 isoforms. Then, the secondary antibody, goat anti-rabbit IgG-HRP conjugate (1:2,000; cat. no. P0448; Dako Denmark, Glostrup, Hovedstaden, DK) was incubated for 3 h at 4˚C. The estimated molecular weight for RHBDD2 isoform A is 39.21 kDa (364 aa), and for RHBDD2 isoform B is 23.64 kDa (223 aa). ACTB was used as a loading reference (42 kDa). It was detected using the primary antibody: mouse anti-β-actin-HRP conjugate (1:5,000; cat. no. ab173838; Abcam, Cambridge, MA, USA) incubated for 3 h at 4˚C. Protein bands were visualized by chemiluminescence reaction on radiographic plates using the EasySee Western Blot kit (DW101-01; TransBionovo, BJ, CN). The relative expression of the RHBDD2 isoforms was determined by density band analysis with ImageJ software (https://imagej.nih.gov/ij/).

RHBDD2 subcellular localization by confocal immunofluorescence. The RHBDD2 subcellular localization was determined by fluorescence immunocytochemistry in MCF7, T47D and MDA-MB-231 cells. Cells were grown on a 100-mm^2 cover glass to 70% confluence and fixed with 4% formaldehyde or cold acetone. Initially, the cell membrane was permeabilized with 0.01% Triton, incubating for 10 min at room temperature. Then, the cells were incubated overnight at 4˚C with the primary antibodies: rabbit anti-RHBDD2 (1:400); mouse anti-CANX (1:50; cat. no. MA3-027; Thermo Fisher Scientific, Inc.) for ER detection (17); mouse anti-GalNacT3 (culture supernatant donated by Professor Ulla Mandel, Copenhagen Center for Glycomics, University of Copenhagen) for Golgi apparatus detection (18); and mouse anti-Ykt6p v-SNARE (E-2) (1:50; cat. no. sc-365732; Santa Cruz Biotechnology, Dallas, TX, USA) for transport vesicle detection (19). Later, cells were incubated for 2 h at 4˚C with the secondary antibodies: goat anti-rabbit IgG-Cy3 conjugate (1:200; cat. no. 711165152; Jackson ImmunoResearch Laboratories, Inc., West Grove, PA, USA) and goat anti-mouse IgG-biotin conjugate (1:100; cat. no. BA9200; Vector Laboratories, Inc.,

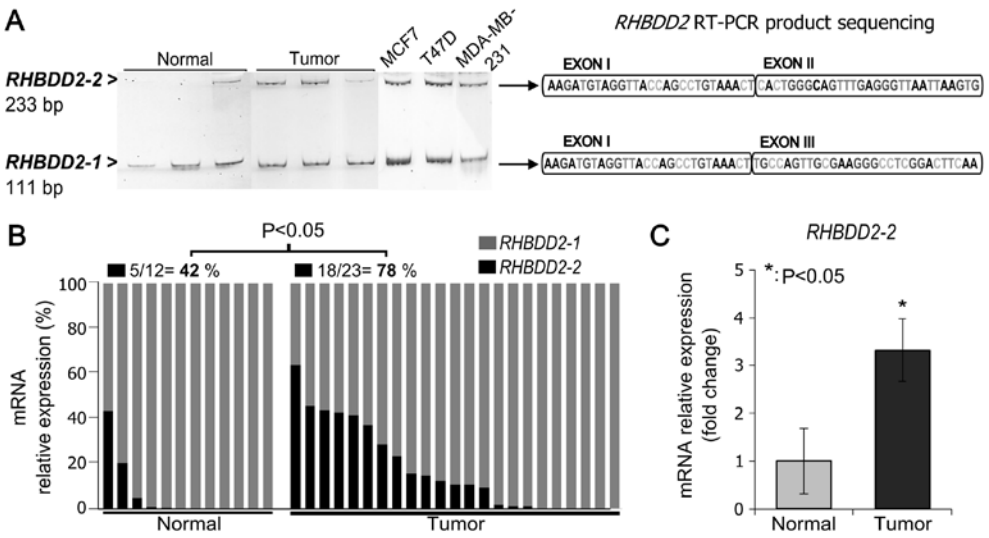

Figure 1. *RHBDD2* splicing variants in tumor and normal breast tissues, and breast cancer cell lines. (A) The identity of the *RHBDD2* splicing variant RT-PCR products was confirmed by sequencing. (B) A significant statistical increased rate of *RHBDD2-2* expression was identified in the tumors (18/23, 78%) when compared to normal breast tissues (5/12, 42%) (P<0.05). (C) A significant statistical increment in *RHBDD2-2* expression level was observed in carcinomas in respect to the normal breast tissues (P<0.05). Error bars: ±2 SD.

Burlingame, CA, USA). Then, the cells were incubated with streptavidin-FITC conjugated-(1:10,000; cat. no. SA10002; Thermo Fisher Scientific, Inc.) for 30 min at room temperature. Finally, cells were visualized using the Confocal FluoView™ 1000 immunofluorescence microscope. Images were acquired at red and green fluorescence signal channels with the associated FluoView Software (Olympus Latin America, Miami, FL, USA). Colocalization analysis was performed with the JaCoP application on ImageJ software. The Pearson's (R) correlation coefficient was calculated for colocalization quantification (20).

Statistical analysis. RT-qPCR experiments were performed in triplicate for each data point. Data were analyzed using the Student's t-test or one-way analysis of variance (ANOVA). Data are expressed as the means ± 2 standard deviations (SDs) of the sample. All tests were two-tailed, and the level of statistical significance was set at P≤0.05. Statistical analysis was performed with R Software (https://www.r-project.org/).

In silico analysis of RHBDD2 splicing variants in breast carcinomas. To further investigate the relevance of both *RHBDD2* splicing variants in human breast carcinomas, *RHBDD2* transcript variant profiles were analyzed employing The Cancer Genome Atlas-Breast Cancer (TCGA-BRCA) RNA-Seq dataset obtained from the UCSC Xena TOIL RNA-seq recompute resource.

Briefly, *RHBDD2-1* (ENST00000006777.10) and *RHBDD2-2* (ENST00000428119.1) expression levels were evaluated in 1,092 primary invasive breast carcinomas. Seven-hundred and twenty-nine cases out of 1,092 showed high expression levels of *RHBDD2-1* (Var 1), *RHBDD2-2* (Var 2) or both variants that were subsequently grouped according to their intrinsic subtypes, proliferative and Risk-Of-Recurrence scores (ROR-P). Intrinsic subtypes and their derivate scores (proliferation and ROR-P) were determined using the 50-gene (PAM50) predictor bioclassifier R script (21).

Results

The RHBDD2 gene encodes two splicing variants differentially expressed in tumor and normal tissues. *RHBDD2* gene sequence analysis allowed the identification of 5 exons and 4 introns with two putative transcripts differentiated by the alternative splicing of exon II in the mature mRNA (4). The *RHBDD*2 mRNA variant 1 (*RHBDD2-1*) is a transcript of 1,756 nt encoded by the exons I, III, IV and V. The *RHBDD2-2* variant is a transcript of 1,878 nt encoded by the exons I, II, III, IV and V.

The expression pattern of the *RHBDD2* splicing variants was evaluated on breast cancer cell lines and on known *RHBDD2*-positive breast tumor and normal samples by RT-PCR. We used a primer pair designed to detect both mRNA variants; the forward primer spanned exon I and the reverse primer spanned exon III. The expected PCR products for the *RHBDD2-1* and *RHBDD2-2* variants (111 bp and 233 bp, respectively) were detected on the analyzed samples. The identity of the amplification products was confirmed by PCR amplicon sequencing (Fig. 1A).

In addition, *RHBDD2* splicing variants expression were analyzed by RT-qPCR in normal and tumor samples (Fig. 1B). *RHBDD2-1* expression was detected in all normal and tumor samples. While, *RHBDD2-2* expression was more frequently detected in tumors (78%, 18 out of 23) than in normal tissues (42%, 5 out of 12) (P<0.05, Fig. 1B). Moreover, a significant increment in the *RHBDD2-2* expression level was detected in tumors in respect to normal breast samples (P<0.05, Fig. 1C).

RHBDD2-2 expression is associated with poor patient prognostic factors. The expression profiles of *RHBDD2* splicing variants were analyzed in a 729 breast cancer samples, obtained from the TCGA-BRCA RNA-Seq database.

RHBDD2-2 variant expression was found to be significantly more frequent in basal-like breast carcinomas (49% of cases) in respect to luminal-like tumors (19% of cases, P<0.05),

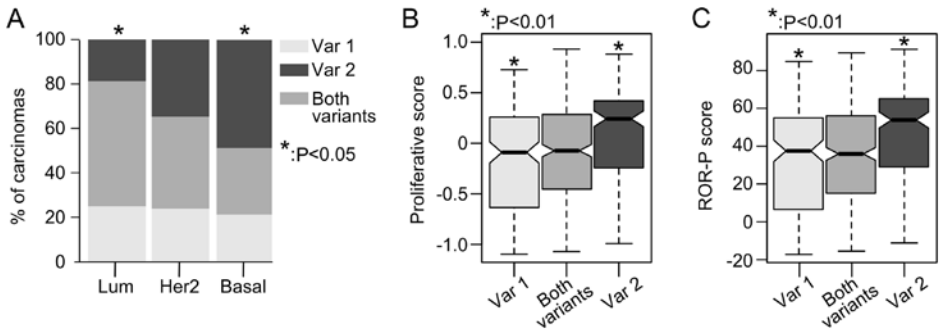

Figure 2. Expression of *RHBDD2* splicing variants in 729 breast cancer samples from the TCGA-BRCA RNA-Seq data set. (A) Increased expression level of *RHBDD2-2* mRNA was detected in the basal-like (Basal) breast cancer subtype in respect to the Her2-enriched (Her2) and the luminal-like (Lum) subtypes. This increment was statistically significant (P<0.05) respect the luminal-like subtype. (B and C) Proliferation and ROR-P scores were found to be higher in those patients who only show *RHBDD2-2* (Var 2) expression, in respect to those who express only *RHBDD2-1* (Var 1) or both splicing variants.

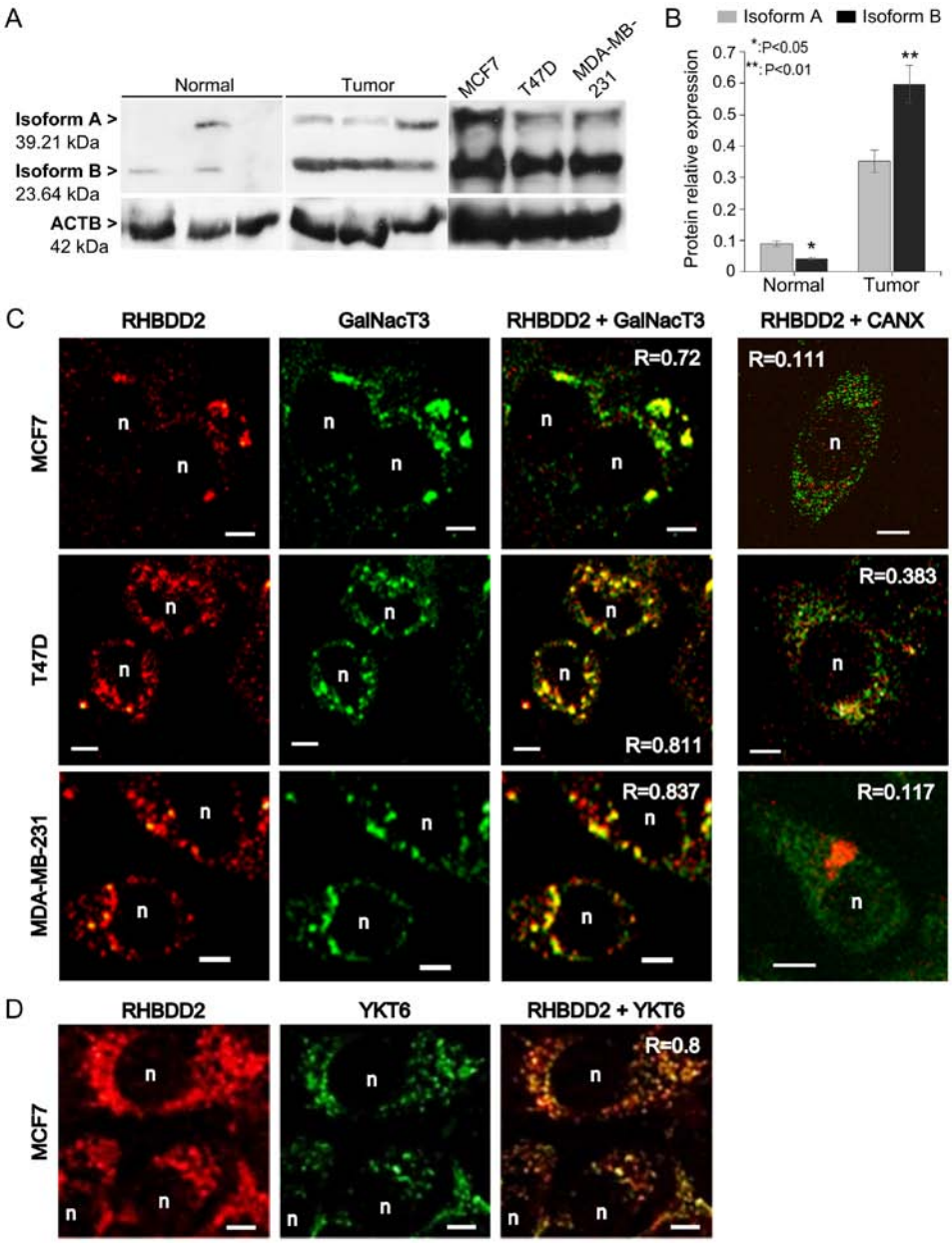

Figure 3. Expression analysis and subcellular localization of RHBDD2 protein isoforms. (A) Western blot analysis of RHBDD2 isoforms and ACTB protein in tumor and normal breast tissues, and breast cancer cell lines. (B) Relative RHBDD2 isoform expression using ACTB as a reference. The expression level of isoform B in respect to isoform A was found to be significantly elevated in tumors (P<0.01), but reduced in normal tissues (P<0.05). Error bars: ±2 SD. (C and D) Confocal immunofluorescence microscopy images. RHBDD2 shows colocalization with GalNacT3 (R>0.7) and YKT6 (R=0.8), but not CANX (R<0.4). Red for RHBDD2. Green for GalNacT3, YKT6, and CANX. Yellow, the colocalization areas. R=Pearson's coefficient. n=nucleus. Scale bars are equivalent to 5 μm.

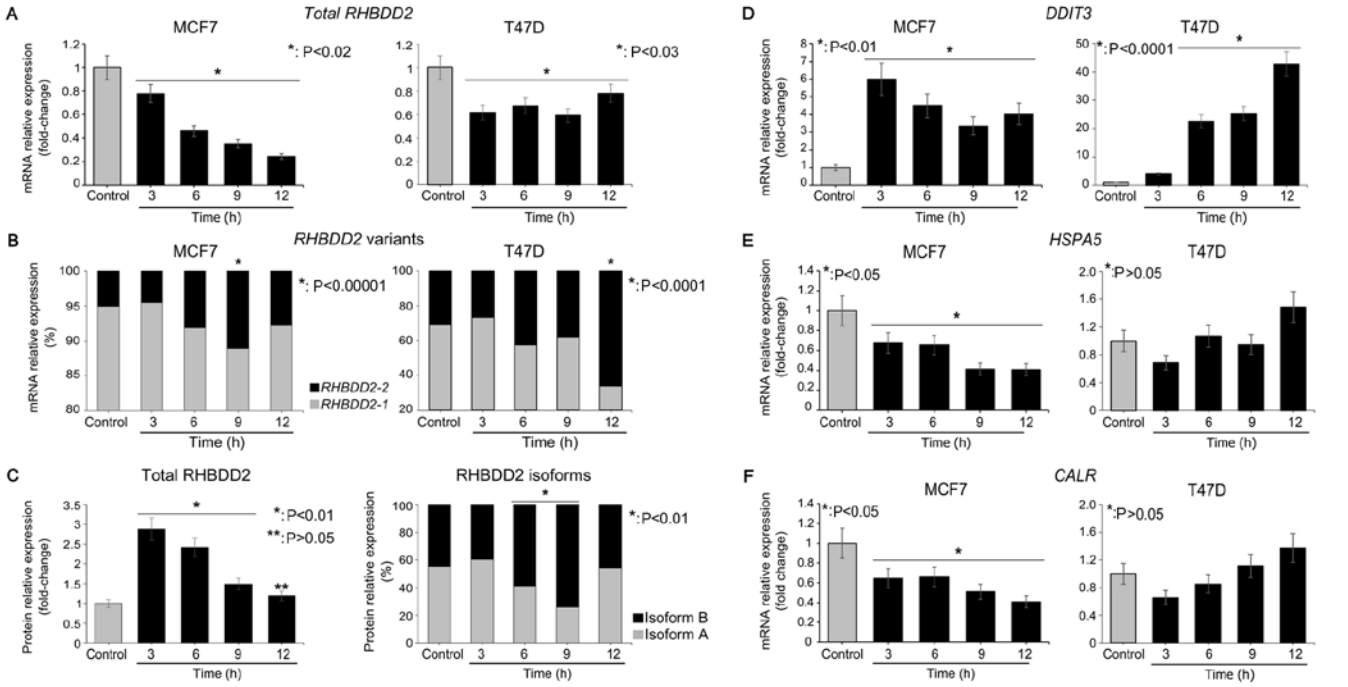

Figure 4. *RHBDD2* expression analysis under glucose starvation conditions. (A) A statistically significant decrease in total *RHBDD2* expression was observed in response to GS in MCF7 (P<0.02) and T47D (P<0.03) cells. (B) A significant *RHBDD2-2* mRNA upmodulation was detected at 6 h of GS in both cell lines (P<0.01), while *RHBDD2-1* variant was downmodulated after GS treatment. (C) RHBDD2 protein isoforms were also evaluated. A significant increment in isoform B expression levels were detected in GS-treated cells at 6 and 9 h (P<0.01) of treatment, with a significant reduction in isoform A (P<0.01). (D) *DDIT3* expression upmodulation was detected in MCF7 (P<0.01) and T47D cells (P<0.0001) in response to GS stress. (E and F) *HSPA5* and *CALR* mRNA levels were analyzed as ER cell stress response biomarkers, demonstrating that GS treatment did not induce ER cell stress response in both cellular models. Error bars: ±2 SD.

but not in respect to Her2-enriched tumors (P>0.05) (Fig. 2A). In addition, patients with primary breast carcinomas that expressed the *RHBDD2-2* variant had an increased proliferative and ROR-P scores compared with tumors expressing the *RHBDD2-1* variant (P<0.01, Fig. 2B and C).

RHBDD2-2 is translated to protein and overexpressed in breast cancer cells. In order to confirm RHBDD2-2 expression at the protein level, total protein from breast cancer cell lines, normal and breast tumor samples was analyzed by western blot. An anti-RHBDD2 antibody against a C-terminus aa sequence present in both RHBDD2 isoforms was used. The *RHBDD2-1* mRNA variant encodes a 364 aa protein known as isoform A (39.21 kDa). The *RHBDD2-2* variant encodes a 223 aa protein we called isoform B protein (23.64 kDa) with a shorter N-terminus, translated from an internal AUG codon in exon III.

Both RHBDD2 protein isoforms were detected: isoform A at 39 kDa and isoform B at 24 kDa. ACTB was used as reference for relative protein isoform amount estimation (Fig. 3A). As expected, a significant overexpression of total RHBDD2 protein was detected in the tumor samples (P<0.01). Individual RHBDD2 isoform analysis detected a statistically significant increment of RHBDD2 isoform B expression in respect to isoform A in the tumoral samples (P<0.01). In contrast, isoform B expression was lower than isoform A in the normal samples (P<0.05, Fig. 3B).

RHBDD2 subcellular localization. RHBDD2 subcellular localization was determined by confocal immunofluorescence microscopy in the human breast cancer cell lines MCF7, T47D and MDA-MB-231. Quantification of colocalization analysis revealed a positive correlation between RHBDD2 and the Golgi apparatus marker GalNacT3 (R>0.7, Fig. 3C), also the ER-Golgi/intra-Golgi transport vesicle marker Ytk6 v-SNARE (R=0.8, Fig. 3D), but not the ER marker CANX (R<0.4, Fig. 3C).

Glucose starvation triggers RHBDD2 variant 2 expression in breast cancer cells. Total *RHBDD2* and *RHBDD2-2* mRNA levels were evaluated in the MCF7 and T47D cells under GS conditions from 3 to 12 h by RT-qPCR. A significant decrease in total *RHBDD2* mRNA expression was detected under GS conditions in the MCF7 (P<0.02) and T47D (P<0.03) cell lines (Fig. 4A). However, a statistically significant induction of *RHBDD2-2* expression was observed at 6 h of GS treatment in both cancer cell lines (P<0.01). The *RHBDD2-2* highest expression levels were detected at 9 and 12 h of GS treatment in the MCF7 (P<0.00001) and T47D (P<0.0001) cells respectively (Fig. 4B). In addition, a concomitant significant *RHBDD2-1* decrease was observed (P<0.03, Fig. 4B), indicating a switch from RHBDD2 variant 1 to RHBDD2 variant 2 in response to GS. The cellular response to GS was confirmed by *DDIT3* mRNA level analysis (13). As expected, a significant increment of *DDIT3* expression was detected under GS in the MCF7 (P<0.01) and T47D (P<0.0001) cells (Fig. 4D). In addition, *CALR* and *HSPA5* mRNA levels were analyzed as ER cell stress response biomarkers (14,15). These data suggest that GS treatment does not induce ER cell stress response in both cellular models (Fig. 4E and F).

Furthermore, expression of RHBDD2 protein isoforms was also analyzed in MCF7 cells. A significant increment of total RHBDD2 protein was detected at 3, 6 and 9 h of GS respect to controls (P<0.01, Fig. 4C). In addition, a significant increment of isoform B expression was detected at 6 and 9 h of GS in respect to the control cells (P<0.01), while a significant reduction of isoform A was observed (P<0.01, Fig. 4C).

Discussion

The *RHBDD2* gene belongs to the Rhomboid transmembrane protein superfamily. Among the rhomboid proteases and pseudoproteases members, *RHBDD2* is classified as a pseudoprotease because of the loss of the catalytic site (1). Although the *RHBDD2* cell function is unknown, its aberrant expression has been associated with malignant diseases (2). *RHBDD2* overexpression was initially described by Abba *et al* in patients with advanced breast cancer as a consequence of gene amplification events (3). Recently, we described a significant association between *RHBDD2* overexpression among breast carcinomas with low/negative progesterone receptor expression (6). In the present study, we demonstrated that *RHBDD2* mRNA variants and their coding proteins can be differentially detected in breast tumor and normal specimens. As previously described (3,4,6), total *RHBDD2* (mRNA and protein) was found to be upregulated in breast carcinomas. However, individual splicing variant analysis allowed us to detect a significant increment in *RHBDD2-2* variant expression in breast carcinomas in respect to normal tissues. More importantly, we identified an increased expression of isoform B in respect to isoform A in tumor samples, extending our previous knowledge of RHBDD2 expression in this malignant disease. Furthermore, *in-silico* analysis of TCGA-BRCA RNA-Seq data showed a significantly increased expression of the *RHBDD2-2* variant in the basal-like breast cancer subtype. This subtype is characterized by an aggressive phenotype and does not respond to hormonal therapy but to chemotherapy with anthracycline and taxane (22). The *RHBDD2-2* variant was also associated with the highest cell proliferation and ROR-P scores indicating a worse outcome for patients with this variant expression in respect to *RHBDD2-1*.

Sustained tumor growth requires the capability to deal with a nutrient-deprived microenvironment before neovascular development. Glucose deprivation has diverse effects in cancer cell lines depending on lineage differences and the presence of mutations in the several pathways it may trigger (23). Besides the alteration in glucose metabolism and cancer-related pathways (eg. mTOR and AKT), glucose starvation may trigger changes in RNA processing, protein delivery and Golgi physiology (24,25). In the present study, we evaluated the *RHBDD2* response to nutritional stress by glucose deprivation based on its previously described association with the modulation of cellular stress conditions (5,7). A decrease in total *RHBDD2* mRNA expression level was detected in response to GS. However, we observed a significant increase in *RHBDD2-2* expression concomitant with a reduction in *RHBDD2-1* mRNA levels. Under normal glucose conditions *RHBDD2-1* was the most expressed variant. In agreement with these data, RHBDD2 protein isoform B significantly increased its expression in response to glucose deprivation in contrast to the isoform A, whose expression was reduced. The mechanisms that could modulate mRNA splicing in response to glucose starvation in *in vitro* models have not been completely determined. Regulation of mRNA splicing by nutritional factors has been described in glucose-6-phosphate dehydrogenase (*G6PD*) expression (24). Starvation inhibits *G6PD* splicing by decreasing the rate of intron removal, leading to a decrease in mature mRNA (26). Glucose starvation-induced splicing regulatory events have also been described in tumor cell lines. In murine ovarian carcinoma cells, *VEGF* mRNA variant expression and stability are affected by glucose starvation (27).

mRNA sequence analysis indicated that protein isoform A is translated from an AUG codon in the *RHBDD2-1* exon I, while isoform B should be translated from an internal AUG codon located in the *RHBDD2-2* exon III. Two well-known stress-related regulatory mechanisms could be driving the translation process of isoform B: the internal ribosome entry sites (IRES) and the upstream open reading frames (uORFs) (28). IRES elements are specialized RNA regulatory sequences governing cap-independent translation initiation from internal AUGs that are translated during cellular stress when cap-dependent translation is compromised (29). uORFs are sequences defined by an initiation codon in frame with a termination codon located upstream or downstream to the main AUG. uORFs has been described to modulate the expression of stress-related mRNAs such as *CHOP*, *ATF4/5* and *GADD34* (30). Importantly, *RHBDD2* mRNA sequence analysis using the IRESite resource (http://iresite.org/) allow us to identify IRES elements in the 5'UTR region of the *RHBDD2-2* variant. These regulatory sequences could be modulating the translational process of the RHBDD2 isoform B under different cellular stress conditions.

Using confocal microscopy, we were able to corroborate the localization of the RHBDD2 proteins at the Golgi apparatus of human breast cancer cells, as was previously determined in mouse-derived cell lines (31,32). We also identified the RHBDD2 proteins associated with V-SNARE transport vesicles involved in different Golgi trafficking processes. Overall, we proposed that a switch in *RHBDD2* splicing variants and its protein products in the Golgi and associated transport vesicles may be related to a pro-survival signaling pathway initiated under the stressful tumor microenvironment conditions. Nevertheless, further studies should be conducted in other cancer cell lines and *in vivo* models in order to corroborate our findings and also to elucidate the role of the *RHBDD2-2* variant in breast cancer progression.

Acknowledgements

The authors thank to Professor Ulla Mandel for antibody donation.

Funding

The present study was supported by the National Agency of Scientific and Technological Promotion (PICT-2015-0149) and The National Cancer Institute of Argentina (INC-MSAL).

Availability of data and materials

The datasets used and/or analyzed during the current study are available from the corresponding author on reasonable request.

Authors' contributions

MCA and RC conceived and designed the study. RC, MER, AG, VF and SP performed the experiments. RC, MCA and EL performed the statistical and bioinformatic analysis. MER, MIL, MVC collect the samples. RC and MCA wrote the paper. RC, MCA, MER and MVC reviewed and edited the manuscript. All authors read and approved the manuscript and agree to be accountable for all aspects of the research in ensuring that the accuracy or integrity of any part of the work are appropriately investigated and resolved.

Ethics approval and consent to participate

All procedures performed in studies involving human participants were in accordance with the ethical standards of the Bioethics Committee of the School of Medical Sciences (COBIMED) from the National University of La Plata, Protocol N° 0800-017399/13-000 and with the 1964 Helsinki Declaration and its later amendments or comparable ethical standards. Informed consent was obtained from all individual participants included in the study.

Consent for publication

Not applicable.

Competing interests

The authors declare that they have no competing interests.

References

1. Freeman M: The rhomboid-like superfamily: Molecular mechanisms and biological roles. Annu Rev Cell Dev Biol 30: 235-254, 2014.
2. Bergbold N and Lemberg MK: Emerging role of rhomboid family proteins in mammalian biology and disease. Biochim Biophys Acta 1828: 2840-2848, 2013.
3. Abba MC, Sun H, Hawkins KA, Drake JA, Hu Y, Nunez MI, Gaddis S, Shi T, Horvath S, Sahin A and Aldaz CM: Breast cancer molecular signatures as determined by SAGE: Correlation with lymph node status. Mol Cancer Res 5: 881-890, 2007.
4. Abba MC, Lacunza E, Nunez MI, Colussi A, Isla-Larrain M, Segal-Eiras A, Croce MV and Aldaz CM: Rhomboid domain containing 2 (RHBDD2): A novel cancer-related gene over-expressed in breast cancer. Biochim Biophys Acta 1792: 988-997, 2009.
5. Lacunza E, Canzoneri R, Rabassa ME, Zwenger A, Segal-Eiras A, Croce MV and Abba MC: RHBDD2: A 5-fluorouracil responsive gene overexpressed in the advanced stages of colorectal cancer. Tumour Biol 33: 2393-2399, 2012.
6. Canzoneri R, Lacunza E, Isla Larrain M, Croce MV and Abba MC: Rhomboid family gene expression profiling in breast normal tissue and tumor samples. Tumour Biol 35: 1451-1458, 2014.
7. Lacunza E, Rabassa ME, Canzoneri R, Pellon-Maison M, Croce MV, Aldaz CM and Abba MC: Identification of signaling pathways modulated by RHBDD2 in breast cancer cells: A link to the unfolded protein response. Cell Stress Chaperones 19: 379-388, 2014.
8. Biamonti G, Catillo M, Pignataro D, Montecucco A and Ghigna C: The alternative splicing side of cancer. Semin Cell Dev Biol 32: 30-36, 2014.
9. Venables JP: Aberrant and alternative splicing in cancer. Cancer Res 64: 7647-7654, 2004.
10. Ghigna C, Valacca C and Biamonti G: Alternative splicing and tumor progression. Curr Genomics 9: 556-570, 2008.
11. David CJ and Manley JL: Alternative pre-mRNA splicing regulation in cancer: Pathways and programs unhinged. Genes Dev 24: 2343-2364, 2010.
12. Oltean S and Bates DO: Hallmarks of alternative splicing in cancer. Oncogene 33: 5311-5318, 2014.
13. Carlson SG, Fawcett TW, Bartlett JD, Bernier M and Holbrook NJ: Regulation of the C/EPB-related gene gadd153 by glucose deprivation. Mol Cell Biol 13: 4736-4744, 1993.
14. Lee AS: The ER chaperone and signalling regulator GRP78/BiP as a monitor of endoplasmic reticulum stress. Methods 35: 373-381, 2005.
15. Michalak M, Groenendyk J, Szabo E, Gold LI and Opas M: Calreticulin, a multi-process calcium-buffering chaperone of the endoplasmic reticulum. Biochem J 417: 651-666, 2009.
16. Livak KJ and Schmittgen TD: Analysis of relative gene expression data using real-time quantitative PCR and the $2^{-\Delta\Delta CT}$ method. Methods 25: 402-408, 2001.
17. Bergeron JJ, Brenner MB, Thomas DY and Williams DB: Calnexin: A membrane-bound chaperone of the endoplasmic reticulum. Trends Biochem Sci 19: 124-128, 1994.
18. Röttger S, White J, Wandall HH, Olivo JC, Stark A, Bennett EP, Whitehouse C, Berger EG, Clausen H and Nilsson T: Localization of three human polypeptide GalNAc-transferases in HeLa cells suggests initiation of O-linked glycosylation throughout the Golgi apparatus. J Cell Sci 111: 45-60, 1998.
19. Zhang T and Hong W: Ykt6 forms a SNARE complex with syntaxin 5, GS28, and Bet1 and participates in a late stage in endoplasmic reticulum-Golgi transport. J Biol Chem 276: 27480-27487, 2001.
20. Bolte S and Cordelières FP: A guided tour into subcellular colocalization analysis in light microscopy. J Microsc 224: 213-232, 2006.
21. Parker JS, Mullins M, Cheang MC, Leung S, Voduc D, Vickery T, Davies S, Fauron C, He X, Hu Z, *et al*: Supervised risk predictor of breast cancer based on intrinsic subtypes. J Clin Oncol 27: 1160-1167, 2009.
22. Dai X, Li T, Bai Z, Yang Y, Liu X, Zhan J and Shi B: Breast cancer intrinsic subtype classification, clinical use and future trends. Am J Cancer Res 5: 2929-2943, 2015.
23. He N, Kim N, Jeong E, Lu Y, Mills GB and Yoon S: Glucose starvation induces mutation and lineage-dependent adaptive responses in a large collection of cancer cell lines. Int J Oncol 48: 67-72, 2016.
24. Amir-Ahmady B and Salati LM: Regulation of the processing of glucose-6-phosphate dehydrogenase mRNA by nutritional status. J Biol Chem 276: 10514-10523, 2001.
25. Hicks SW and Machamer CE: Golgi structure in stress sensing and apoptosis. Biochim Biophys Acta 1744: 406-414, 2005.
26. Cyphert TJ, Suchanek AL, Griffith BN and Salati LM: Starvation actively inhibits splicing of glucose-6-phosphate dehydrogenase mRNA via a bifunctional ESE/ESS element bound by hnRNP K. Biochim Biophys Acta 1829: 905-915, 2013.
27. Zhang L, Conejo-Garcia JR, Yang N, Huang W, Mohamed-Hadley A, Yao W, Benencia F and Coukos G: Different effects of glucose starvation on expression and stability of VEGF mRNA isoforms in murine ovarian cancer cells. Biochem Biophys Res Commun 292: 860-868, 2002.
28. Spriggs KA, Bushell M and Willis AE: Translational regulation of gene expression during conditions of cell stress. Mol Cell 40: 228-237, 2010.
29. Martínez-Salas E, Piñeiro D and Fernández N: Alternative mechanisms to initiate translation in eukaryotic mRNAs. Comp Funct Genomics 2012: 391546, 2012.
30. Barbosa C, Peixeiro I and Romão L: Gene expression regulation by upstream open reading frames and human disease. PLoS Genet 9: e1003529, 2013.
31. Ahmedli NB, Gribanova Y, Njoku CC, Naidu A, Young A, Mendoza E, Yamashita CK, Ozgül RK, Johnson JE, Fox DA and Farber DB: Dynamics of the rhomboid-like protein RHBDD2 expression in mouse retina and involvement of its human ortholog in retinitis pigmentosa. J Biol Chem 288: 9742-9754, 2013.
32. Ferretti VA, Canzoneri R, Barbeito CG, Croce MV, Abba MC and Lacunza E: Spatiotemporal expression of Rhomboid domain containing 2 (Rhbdd2) during rat development. Acta Histochem 117: 635-641, 2015.